

Published in final edited form as:

Cell Rep. 2012 July 26; 2(1): 136–149. doi:10.1016/j.celrep.2012.06.005.

Age-related Oxidative Stress Compromises Endosomal Proteostasis

Elvira S. Cannizzo^{1,6}, Cristina C. Clement¹, Kateryna Morozova¹, Rut Valdor¹, Susmita Kaushik², Larissa N. Almeida^{1,7}, Carlo Follo^{1,6}, Ranjit Sahu¹, Ana Maria Cuervo^{2,4}, Fernando Macian^{1,4}, and Laura Santambrogio^{1,3,4,5}

¹Department of Pathology, Albert Einstein College of Medicine, Bronx, NY, 10461, USA.

²Department of Developmental and Molecular Biology, Albert Einstein College of Medicine, Bronx, NY, 10461, USA.

³Department of Microbiology and Immunology, Albert Einstein College of Medicine, Bronx, NY, 10461, USA.

⁴Institute for Aging Research, Albert Einstein College of Medicine, Bronx, NY, 10461, USA.

Abstract

A hallmark of aging is an imbalance between production and clearance of reactive oxygen species and increased levels of oxidatively damaged biomolecules. Herein we demonstrate that splenic and nodal antigen presenting cells purified from old mice accumulate oxidatively modified proteins with side chain carbonylation, advanced glycation end products and lipid peroxidation. We show further that the endosomal accumulation of oxidatively modified proteins interferes with the efficient processing of exogenous antigens and degradation of macroautophagy-delivered proteins. In support of a causative role for oxidized products in the inefficient immune response, a decrease in oxidative stress improved the adaptive immune response to immunizing antigens. These findings underscore a previously unrecognized negative effect of age-dependent changes in cellular proteostasis on the immune response.

Introduction

Reactive oxygen species (ROS) are molecules in which the outer electron orbital holds one or two unpaired electrons. Among these, hydrogen (H[•]), hydroxyl radical (OH[•]), transition metals (copper and iron), oxygen (O[•] and RO[•]), diatomic oxygen (O₂[•], H O₂[•] R O₂[•]), and its superoxide (O₂^{•-}) are the most abundant species (Halliwell et al., 2009; Hamanaka et al., 2010; Wellen et al., 2010; Cannizzo et al., 2011). ROS are physiologically produced by all cells and mostly derived from leakage of the electron transport chain in mitochondria (Barjia et al., 2000; Dufour et al., 2000; Starkov et al., 2004; Lin et al., 2006; Chandel et al., 2010; Cannizzo et al., 2011). In inflammatory cells a second important source of ROS production is the “oxidative burst,” where the NADPH oxidase complex catalyzes the formation of

© 2012 Elsevier Inc. All rights reserved.

⁵ Corresponding author: Laura Santambrogio: Albert Einstein College of Medicine, 1300 Morris Park Avenue, Bronx, NY 10461. laura.santambrogio@einstein.yu.edu Tel, 718 430-3458.

⁶Current address: Department of Medical Sciences, University of Piemonte Orientale Medical School, Novara, Italy

⁷Current address: Instituto de Biofísica Carlos Chagas Filho, Universidade Federal do Rio de Janeiro

Publisher's Disclaimer: This is a PDF file of an unedited manuscript that has been accepted for publication. As a service to our customers we are providing this early version of the manuscript. The manuscript will undergo copyediting, typesetting, and review of the resulting proof before it is published in its final citable form. Please note that during the production process errors may be discovered which could affect the content, and all legal disclaimers that apply to the journal pertain.

diatomic oxygen and the enzymes myeloperoxidase and bromoperoxidase catalyze the formation of hypochlorite (ClO^-), hypochlorous acid (HOCl) and hypobromous acid (HOBr) as an innate immune mechanism to eradicate pathogens (Park 2003; Cathcart 2004; Klebanoff 2005; Dale et al., 2008). Since ROS are unstable molecular species which can readily induce the non-enzymatic oxidation of biomolecules, cells are equipped with a series of enzymes that include different isoforms of superoxide dismutase, catalase, peroxiredoxin and glutathione peroxidase, to readily dispose of ROS (Johnson et al., 2005; Roberts et al., 2009; Chandel et al., 2010; Haigis et al., 2010; Wellen et al., 2010; Cannizzo et al., 2011). In aging cells an imbalance due to increased ROS production and a decrease in the levels and activity of the ROS-converting enzymes, leads to the non-enzymatic oxidation of proteins, carbohydrates, lipids and nucleic acids, a process generally known as oxidative stress (Broadley et al., 2008; Alexeyev 2009; Halliwell et al., 2009; Roberts et al., 2009; Hamanaka et al., 2010; Wellen et al., 2010; Cannizzo et al., 2011; Durieux et al., 2011).

The mechanism(s) for clearance of oxidized proteins depends on the sub-cellular localization of the protein, the level of oxidation and the nature of the specific oxidized amino acid. Mildly oxidized cytosolic proteins are degraded by the proteasome system in an ubiquitin dependent or independent fashion or by a selective form of lysosomal degradation known as chaperone-mediated autophagy (CMA) (Dunlop et al., 2009; Cuervo et al., 2010; David et al., 2010; Tyedmers et al., 2010). For these proteins the low degree of oxidation still allows for the protein to be unfolded, which is a requirement for entry into the narrow catalytic chamber of the proteasome or the translocation channel that mediates substrate internalization into lysosomes via CMA (Dunlop et al., 2009; Cuervo et al., 2010; David et al., 2010). In contrast, proteins with extensive oxidative damage that cannot unfold are often organized into cytosolic insoluble protein aggregates that are no longer amenable for degradation through these systems. Two distinct aggregating compartments have been described in yeast, one for proteins that can disaggregate and be delivered to the proteasome for degradation and a different compartment for those that are irreversibly aggregated (Kaganovich et al., 2008; Kopito 2000). The generally accepted mechanism for the degradation of these irreversibly aggregated protein inclusions is macroautophagy, a high-capability pathway that delivers cytosolic material to lysosomes inside double membrane vesicles or autophagosomes (Cuervo et al., 2005). Cargo-recognition molecules such as p62 and NBR1 sequester aggregated proteins inside autophagosomes through a selective form of macroautophagy known as aggrephagy (Lamark et al., 2009). For other types of protein aggregates, recruitment of cytosolic chaperones to the aggregate acts as a trigger for their degradation through a macroautophagy variant known as chaperone-assisted selective autophagy (CASA) (Arndt et al., 2010). Late endosomes and lysosomes are the final destination of these aggregate materials after fusion with the autophagosome carriers (Cuervo et al., 2005). In addition, extracellular aggregates organized as amyloid-like structures can also reach late endosomes and lysosomes of tissue resident macrophages and dendritic cells (DC) after being phagocytosed (Chiti et al., 2006; Alvarez et al., 2011; Devitt et al., 2011).

In endosomes/lysosomes most of the damaged biomolecules are degraded to their constitutive basic components by acidic hydrolases (Stern et al., 2006). However, the nature of the oxidized amino acid has an impact on protein turnover in that o- and m-tyrosines increase protein catabolism whereas proteins with dopa modifications are inefficiently degraded and tend to generate high-molecular weight SDS-stable aggregates (Dyer et al., 1993; Oliver et al., 1987; Requena et al., 2001; Dalle-Donne et al., 2003; Isom et al., 2004; Dunlop et al., 2008; Dunlop et al., 2009; Madian et al., 2010). These aggregates can then enlarge by entanglement with non-oxidatively damaged proteins, furthering cellular toxicity (Squier et al., 2001; Cowan et al., 2003; Terman, 2006).

The increased level of free radicals reported in aging cells includes cells of the immune system (de la Fuente et al., 2004; Larbi et al., 2004; Nomellini et al., 2008). Additionally, a decreased level/functionality of the enzymes involved in clearance of free radicals, including catalase and glutathione peroxidase, has also been reported in aged immune cells (Fujimoto et al., 2010). The oxidative post-translational modifications occurring on several proteins have been associated with compromised phagocytosis, proteasomal activity and TLR signaling (Ponnappan et al., 2007; Shaw et al. 2010; West et al., 2010). In aging T cells, oxidative stress has been linked to increased protein carbonylation and glutathionylation of several cytoskeletal, ribosomal and enzymatic proteins, with overall decreased cell functionality (Preynat-Seauve et al., 2003; Larbi et al., 2007; Hung et al., 2010). Finally, oxidative damage to adaptors of the TCR signal transduction machinery has been associated with a decrease in the intensity and length of the activation signal following TCR engagement in aging T cells (Larbi et al., 2004; Larbi et al., 2007).

An aspect of immunosenescence that has not been investigated is whether age-related oxidative stress also compromises the biological functions of dendritic cells (DC) and in particular, the ability of DC to process and present MHC class II restricted antigens. As such, the goal of our analysis was twofold: firstly to qualitatively and quantitatively analyze the presence of oxidatively damaged proteins in DC from aging mice, and secondly to investigate whether oxidative stress interferes with MHC class II restricted presentation and the overall ability to mount an effective immune response.

Results

Accumulation of oxidatively damaged proteins in DC from aging lymphatic organs

A hallmark of aging is an imbalance between production and clearance of ROS, as well as the intra and extracellular accumulation of their byproducts namely oxidized proteins, advanced glycation end (AGE) products and lipid oxidation products (Oliver et al., 1987; Dyer et al., 1993; Barjia et al., 2000; Dufour et al., 2000; Dalle-Donne et al., 2003; Starkov et al., 2004; Lin et al., 2006; Terman, 2006; Halliwell et al., 2009; Chandel et al., 2010; Hamanaka et al., 2010; Madian et al., 2010; Wellen et al., 2010; Cannizzo et al., 2011). Oxidatively damaged biomolecules have been shown to compromise cellular functions in several dividing and non-dividing cells (Preynat-Seauve et al., 2003; de la Fuente et al., 2004; Larbi et al., 2004; Larbi et al., 2007; Ponnappan et al., 2007; Nomellini et al., 2008; Fujimoto et al., 2010; Hung et al., 2010; West et al., 2010). However, whether byproducts of oxidative stress accumulate in primary and secondary lymphatic organs and whether their possible accumulation affects the ability of DC to mount an adaptive immune response is currently unknown.

To address this question we isolated CD34⁺ bone marrow precursors; the progenitor cells that give rise to several of the hematopoietic cell lineages including DC. CD11c⁺ conventional DC were also isolated from different lymphatic organs, including bone marrow, spleen and peripheral lymph nodes, or cultured from bone marrow precursors derived from 3, 12 and 22 months old mice. The presence of oxidative damage in CD34⁺ cells would indicate that DC precursors are already compromised in their cellular proteome and likely give rise to functionally less efficient DC.

To test for the presence of oxidatively damaged proteins, total cell lysates were incubated with 2,4-dinitrophenylhydrazine (DNPH), which selectively binds to carbonyl groups (ketone or aldehyde) that are added to amino acids side chains as an oxidative irreversible modification. Lysates were run on a 4-15% gradient SDS-PAGE and the blotted membrane developed using an anti-DNPH mAb. Oxidatively carbonylated proteins could be detected in cells derived from all age mice groups, albeit at much higher levels in aging mice (Figure

1a, 1b, 1c, 1d, 1e, 1f, Supplement Figure 1). Interestingly, increased age-related protein carbonylation was observed in CD34⁺ isolated bone marrow cells and conventional DC cultured from bone marrow precursors, indicating that in aging mice even precursor cells or newly differentiated DC accumulate biomarkers of oxidative stress (Figure 1a, b). Besides carbonylation, an increased amount of lipoxidation was also observed in old mice, as detected by probing for malondialdehyde, a highly reactive compound derived from the oxidative degradation of polyunsaturated lipids (Figure 1f).

In order to qualitatively analyze protein carbonylation, DNPH-bound proteins were immunoprecipitated from splenic CD11c⁺ DC purified from 22 month old mice and MS/MS analysis was employed to map oxidized proteins (Figure 1g). As anticipated, oxidized proteins were derived from both intracellular and extracellular sources (Figure 1g, Supplement Table 1 and Supplement Table 2). The former originated from oxidatively damaged organelles, nuclear proteins, cytosolic proteins and the plasma membrane. The latter derived from phagocytosed oxidatively damaged extracellular matrix proteins (Figure 1g and Supplement Table 1). Ingenuity pathway analysis (IPA) was performed to determine the major networks associated with the oxidized proteome. Major pathways included enzymes involved in glycolysis, lipolysis, DNA repair, mitochondrial oxidative phosphorylation, extracellular tissue damage and immunological functions. Taken together, the data indicate that the oxidative proteome could potentially interfere with several cellular biological functions.

Accumulation of oxidatively damaged proteins in endosomal compartments of aging DC

We then mapped the modifications of amino acid side chains generated by ROS, since it is known that individual oxidized species can target proteins for premature degradation or accumulation. For example, hydroxyl or carbonyl modifications on some amino acids generates stable carbonylated proteins which are targeted for proteolysis, whereas hydroxyl attack on tyrosine or phenylalanine generates DOPA, which is a reactive species capable of further modifications including amplification of the oxidative damage to neighboring molecules (Dyer et al., 1993; Requena et al., 2001; Guptasarma et al., 2002; Sacksteder et al., 2006; David et al., 2010; Toda et al., 2010). Amino acids from the immunoprecipitated proteins fragmented by MS/MS (Supplement Table 1) were analyzed for oxidative post-translational modifications. Only residues known to be primary targets of oxidation were analyzed (Table 1). Oxidative moieties comprised a large range of hydroxyl and carbonyl modifications (aldehyde and ketonic groups) and advanced glycation end (AGE) products (Table 1). Additionally, 18% of phenylalanines and 7% of tyrosines were modified to generate DOPA, a moiety known to induce protein aggregation and accumulation into misfolded, protease resistant high molecular weight aggregates (Table 1). Tryptophan, methionine and cysteine have also been reported to undergo oxidation during aging (Requena et al., 2001; Squier et al., 2001; Guptasarma et al., 2002; Dalle-Donne et al., 2003; Madian et al., 2010; Toda et al., 2010), and our results for DC derived from 22 month old mice were consistent with these finding. Tryptophan was found to be oxidized to hydroxykynurenin (4%), oxolactone (16.5%) and kynurenin (13.5%), in addition to the hydroxyl and dihydroxy species (40%), showing that more than 70% of this amino acid was in the oxidized state. Methionine was oxidized to met-sulphoxide (30.1%) and sulfones (20.1%). Cysteine underwent oxidation to cysteine sulfinic acid (dioxidation) (34.7%) and cysteic acid (trioxidation) (31.5%). Thus, more than 60% of tryptophan, methionine and cysteine were shown to be in the oxidized forms. Other oxidations on arginine, lysine, proline and histidine were found to be between 50 to 60%. Histidine and asparagine displayed a lower level of oxidation (15-20 %) (Table 1). Altogether the data support advanced oxidation of the DC proteome in 22 month old mice.

Often protein aggregates can form covalent bonds through Schiff base formation, which involves the interaction of a side chain amine group with a carbonyl group. To determine the presence of high molecular weight protein aggregates, lysates of CD11c⁺ splenic DC from 3, 12 and 22 month old mice were fractionated by gel filtration (Figure 2a). Before separation, proteins were incubated with 2,4-dinitrophenylhydrazine (DNPH) to label the oxidized moieties. This procedure involves incubation in 6% SDS at pH 2, which can disentangle protein aggregates unless they have formed covalent bonds. Since our goal was to detect possible high molecular weight protein aggregates, the samples were run on an S-300 HR sephacryl gel column. Dextran blue (MW of 2×10⁶ kDa) was run as a high molecular weight marker (Figure 2a). Protein micro-aggregates could be detected around 1-3 million kDa (Figure 2a, 2b). Fractions collected before and around the dextran blue elution time were run on an SDS-PAGE and blotted for protein carbonylation. In all age groups oxidized proteins formed micro-aggregates in the high molecular weight range. However, in young mice the aggregates were mostly transient and were solubilized by SDS, which did not occur in older mice (Figure 2b).

Most oxidatively damaged proteins present in the cytosol are processed through the proteasome or by CMA. However, heavily oxidized proteins that cannot unfold in order to enter the catalytic chamber of the proteasome or the translocation complex at the lysosomal membrane, are transported to endosomal/lysosomal compartments by macroautophagy (Kopito, 2000; Kaganovich et al., 2008; Cuervo, 2010). Likewise, oxidatively damaged extracellular proteins, amyloid-like aggregates and oxidatively damaged apoptotic cells are normally phagocytosed by tissue resident macrophages and DC (Chiti et al., 2006; Alavez et al., 2011; Devit et al., 2011). Thus, we determined whether accumulation of oxidatively damaged proteins could be observed in endosomal compartments of DC. To this end, splenic CD11c⁺ DC were generated from 3, 12 and 22 month old mice (previously injected with B16-FLT3-L to expand the DC populations) and late endosomes separated over a 27/10 percoll gradient. As described above, endosomal proteins were incubated with 2,4-dinitrophenylhydrazine (DNPH) to label the oxidized moieties, before separation over a 4-15% SDS-PAGE. Increased amounts of oxidatively damaged proteins could be observed in the endosomes of old mice compared with 3 month old mice (Figure 2c).

Accumulations of lipofuscin aggregates are often observed with age in the endosomes of non-dividing cells such as neurons, cardiomyocytes and endothelial cells. To determine whether lipofuscin accumulation occurred in aging DC, ultrastructural analysis of MHC II immunogold labeled late endosomes was performed using two different Abs specific for I-A^b (Figure 2d). No lipofuscin deposits could be observed in these compartments in aging mice (Figure 2d). This is consistent with the notion that large aggregates only form in non-dividing cells or cells with a very long life span, such as neurons, endothelial cells and cardiomyocytes, where protein/lipid/carbohydrate aggregates form black lipofuscin inclusions, often of considerable size. DC, even in old mice, have a turnover of 7-14 days, thus accumulation of protein aggregates following oxidative stress does not result in the formation of visible lipofuscin inclusions (Figure 2d).

Altered autophagy in aging DC

The accumulation of oxidatively damaged proteins in endosomal compartments of aging DC prompted us to determine whether the sequestration and degradation capability of these compartments could be compromised. To this goal we determined the rates of intracellular proteolysis in splenic DC (CD11c⁺) from 3, 12 and 22-month mice after labeling for 2 days with [³H]-leucine. During the 20h chase cells were maintained in the presence or absence of a combination of ammonium chloride and leupeptin, to block total lysosomal degradation (Figure 3a), or the PI3K inhibitor 3-methyladenine (3MA), widely used to inhibit macroautophagy (Figure 3b). These studies revealed a statistically significant decrease in

total lysosomal degradation as well as basal 3MA-sensitive degradation in aging cells (Figure 3a, 3b).

To analyze further changes in macroautophagy activity with age in DC, we directly measured the total amount and overall processing efficiency of the light chain protein type 3 (LC3), a structural component of autophagosomes that undergoes degradation when these compartments fuse with lysosomes and late endosomes. Immunostaining for LC3 in CD11c⁺ DC purified from the spleen of 3, 12 and 22 month old mice was used to visualize autophagosomes as LC3-positive fluorescent puncta by fluorescence microscopy with deconvolution. As shown in Figure 3c and 3d, the number of autophagosomes per cell was significantly increased in DC in an age-dependent manner. An increase in autophagosome content can result from enhanced formation or decreased clearance of these compartments. To discriminate between these possibilities, we analyzed the LC3 flux by comparing levels of LC3-II, the autophagosome-associated form of the protein, in cells maintained in presence or absence of inhibitors of lysosomal proteolysis. Immunoblot analysis of LC3-II in these experiments confirmed higher steady-state content of autophagosomes in old DC (levels of LC3-II in untreated cells) (Figure 3 e, 3f). In contrast, LC3-II flux was severely compromised in DC from both 12 and 22 month old mice, suggesting inefficient clearance of autophagosomes (Figure 3g). Consistent with the reduced rates of LC3 degradation, we also observed a moderate increase in total cellular levels of p62, a common autophagic cargo, although only at the most advanced ages (Supplement Figure. 2). Levels of beclin 1, involved in initiation of autophagosome formation, and of Atg5, an essential component for the elongation of the autophagosome membrane, markedly increased with age in DC (Supplement Figure 2). These results support the conclusion that induction and formation of autophagosomes is preserved until a late age in DC, and that one of the major steps altered in this process is the clearance of the autophagocytosed material.

Degradation of the autophagosome content can occur through fusion to both late endosomes and lysosomes. Under normal conditions, most cells favor autophagosome fusion with secondary lysosomes, as this compartment has a higher proteolytic capability; however, different reports support the conclusion that cells respond to compromised lysosome-autophagosome fusion by increasing fusion of autophagosomes with late endosomes to form a compartment described as amphisome. Analysis of the colocalization of cytosolic autophagic cargo (mitochondria) or structural autophagosome components (LC3) with the endocytic compartment (by assessing endocytosis of fluorescently labeled BSA), revealed a higher coincidence of these autophagosome and late endosomal markers in DC of older animals (Figure 3h, 3i). These results indicate a higher macroautophagy-mediated transfer of cytosolic material, likely including oxidized micro-aggregated proteins, to the endosomal compartment of DC with age and slower degradation of the cytosolic cargo in these compartments.

DCs from aging mice have a decreased *in vitro* and *in vivo* ability to process exogenously administered antigen

In the next series of experiments, we set to determine whether cellular oxidative stress and accumulation of oxidatively damaged proteins in endosomal organelles compromised MHC II restricted immune responses. To determine whether the reduced proteostasis would compromise adaptive immune responses 3, 12 and 22 month old C57BL/6 (I-A^b) mice were injected in the flanks with 50 micrograms of E α -RFP protein. Six or twelve hours later CD11c⁺ DC were purified from the inguinal draining lymph nodes of each age group and the amount of MHC class II (I-A^b) loaded with the E α 52-68 peptide analyzed by surface staining using the conformational Ab Y-Ae (Figure 4a). A significant decrease in the amount of MHC class II/E α 52-68 loaded complexes was observed on the plasma membrane of DC from 22 and 12 month old mice as compared to 3 month old mice, even

when normalized to the total amount of MHC II molecules and MHC II-CLIP loaded molecules (Figure 4a, 4b, 4c).

To determine whether such differences in antigen presentation could also be observed following immunization, 3, 12 and 22 month old C57BL/6 (I-A^b) mice were injected in the flanks with 100 micrograms of E α -RFP protein in CFA. Two weeks later CD11c⁺ DC were purified from the draining lymph nodes of each age group and the amount of MHC class II (I-A^b) loaded with the E α 52-68 peptide analyzed by surface staining using the conformational Ab YAe (Figure 4d). Again, a significant decrease in the number of DC displaying MHC class II/E α 52-68 loaded complexes was observed on DC from 22 and 12 month old mice as compared to 3 month old mice (Figure 4d). As expected, a decreased surface amount of I-A^b loaded with the E α -RFP 52-68 peptide resulted in a diminished T cell proliferative response (Figure 4e). Supporting an intrinsic defect in DC functions in old mice, decreased proliferation was also observed when DC from 12 and 22 month old mice were incubated with 3 month old T cells (Supplement Figure 3). To further quantify the E α -RFP 52-68 peptide loaded on I-Ab from nodal DC, MHC II eluted peptides were subjected to MS analysis (Figure 4f, 4g). Quantification of the eluted peptides was achieved by spiking the samples with known amounts of monoisotopic labeled E α -RFP 52-68 peptide (Figure 4f, 4g). The E α -RFP 52-68 peptide envelope was easily detected in the mixture of peptides eluted from DC purified from 3 month old immunized mice (Figure 4f). MS/MS fragmentation confirmed the correct peptide sequence (Figure 4g) and a comparison with the standard peptide allowed us to quantify its amount, varying between 31 and 125 femtomoles in two separate experiments (Figure 4f). The amount of E α -RFP 52-68 eluted from 22 month old mice was below our level of detection.

To confirm these results in an additional antigen system, CD11c⁺ splenic DC were purified from 3, 12 and 22 month old CBA mice and pulsed for one and a half hour with forty micrograms of FITC-conjugated HEL (HEL-FITC). Processing of phagocytosed HEL-FITC was monitored by FACS analysis, as disappearance of the FITC fluorescence and by appearance of positive staining for a conformational Ab (AW3.1), specific for I-A^k loaded with the HEL 48-61 peptide (Figure 5a). A lower amount of AW3.1 staining was observed in both 12 and 22 months old mice at each time point as compared to 3 months old mice (Figure 5a). On the other hand, a higher amount of unprocessed HEL-FITC was also observed in aging mice as compared to the 3 months old (Figure 5a).

Differences observed in the amount of E α -RFP processing among the three age groups could be partially related to a differential rate of protein phagocytosis or endosomal trafficking. To control for this possibility, late endosomes were prepared from splenic DC purified from 3, 12 and 22 month old mice (previously injected with B16-FLT3-L to expand the DCs populations) using a 10/27 Percoll gradient (Figure 5b). Purified organelles were then incubated with 5 μ g of E α -RFP and the amount of overall processing analyzed by silver staining at different time points (Figure 5c). In agreement with the antigen processing and presentation assay on intact cells, an increased amount of non-processed protein following digestion was observed for organelles prepared from 12 and 22 month old mice as compared with 3 month old (Figure 5c, 5d). Mass spectrometry analysis performed on E α -RFP peptides isolated from the organelles following protein digestion confirmed a decreased number of E α -RFP specific peptides in 12 and 22, as compared to 3 month old mice (figure 5e). As expected from the equal surface amount of MHC class II among the three age groups, no differences in peptide loading were observed when the pre-processed peptide was added exogenously (Figure 5f). Taken together the data indicate a compromised ability of antigen processing and presentation in DC purified from aging mice.

In the next series of experiments we asked whether decreased proteolytic activity could be the reason for decreased antigen processing observed in aging DC. Total cell lysates from splenic CD11c⁺ DC purified from 3, 12 and 22 month old C57BL6 mice were analyzed by western blotting for cathepsin L and S, and the interferon- γ -inducible lysosomal thiol reductase (GILT). No differences were observed in the total amount of enzymes among the three groups of mice as compared to the LAMP-1 loading control (Supplement Figure 4a). When endosomal proteolytic activity was quantified by flow cytometry, using a cysteine protease specific probe (Cathepsin B, L, and S) which only targets the active form of these enzymes, a similar amount of fluorescence was observed in 12 and 22 month DC, as compared with the 3 month old (Supplement Figure 4b). These data indicate that the altered endosomal proteostasis observed in aging DC is not related to impaired level or activity of endosomal cathepsins. Data are consistent with that previously observed in aging neurons, where engorgement of endosomal compartments with oxidatively damaged proteins induced a decrease in processing activity, despite an increase in the amount of active cathepsins (Takahashi et al., 2007).

In vivo decrease of oxidative stress ameliorates MHC class II restricted immune response to immunizing antigen

In the final series of experiments, we aimed to determine whether a cellular decrease in oxidative stress would increase the ability of DC to process and present the immunodominant E α -RFP 52-68 peptide following in vivo immunization with E α -RFP. To this end 22 month old mice were immunized subcutaneously with 100 μ g of E α -RFP and treated with one intraperitoneal injection of the anti-oxidant pyrrolidine dithiocarbamate (PDTC) at the time of immunization as well as daily in the drinking water for fourteen days. Two weeks following immunization CD11c⁺ DC were purified from the draining lymph nodes and total proteins run on a SDS-PAGE. A decreased amount of high molecular weight micro-aggregates was observed in the treated samples (Figure 6a). Similarly, a decreased amount of DNPH detectable oxidized proteins could be observed following the in vivo treatment (Figure 6b). Importantly, the decrease in the overall amount of oxidative stress up-regulated the amount of surface Y-Ae staining (specific for I-Ab-E α -RFP 52-68) in 22 month old mice (Figure 6c and 6d). Similarly, T cell proliferative responses were partially restored, as indicated by an increase in the stimulation index, in immunized PDTC-treated mice when compared to the untreated controls (Figure 6e).

Importantly, as it has been reported in different systems, whereas the antioxidant activity of PDTC restored biological functions in aging cells, it had the opposite effects on cells from young mice (Supplement Figure 5). This suggests that in aging cells the accumulated amounts of oxidized proteins are the major target for the redox activity of PDTC, whereas in young cells where there is a much lower amount of oxidized molecular targets, PDTC interferes with the cellular redox system which is pivotal to several biological activities (Supplement Figure 5).

Discussion

Oxidative stress is a biological phenomenon which follows a biochemical imbalance between the formation and clearance/buffering of free radicals (Roberts et al., 2009; Haigis et al., 2010). Oxidative stress is a common occurrence in cell biology; as such each organism is equipped with a variety of enzymes which specifically dispose of free radicals (Halliwell et al., 2009; Chandel et al., 2010; Hamanaka et al., 2010; Wellen et al., 2010; Cannizzo et al., 2011). However, in aging an increased production of ROS coupled with a decreased ability of the cell to dispose of them will often induce a chronic level of oxidative stress (Barjia et al., 2000; Dufour et al., 2000; Lin et al., 2006; Roberts et al., 2009; Haigis et al., 2010; Cannizzo et al., 2011). The increased amount of highly reactive free radicals

induces oxidative protein modifications, including direct amino acid oxidation with formation of carbonyl derivatives (aldehyde and ketonic groups on amino acid side chains), or indirect amino acid modifications by addition of peroxidated lipids or products from glycation and glycooxidation (Requena et al., 2001; Guptasarma et al., 2002; Sacksteder et al., 2006; Hung et al., 2010; Toda et al., 2010).

Oxidative modifications often result in protein fragmentation, dissociation, unfolding, exposure of hydrophobic residues and aggregation, and an overall loss of protein function (Dunlop et al., 2009; David et al., 2010; Tyedmers et al., 2010). When the oxidative damage is too extensive and irreversible, proteins are targeted for degradation. Two major factors determine the clearance of oxidized proteins: the overall amount of oxidized molecules, and their level of oxidation. Mildly oxidized cytosolic proteins are almost entirely degraded by the proteasome system and CMA, since a low degree of oxidation still allows protein to unfold and enter the narrow proteasome catalytic chamber or the translocation lysosomal complex (Kopito, 2000; Kaganovich et al., 2008; Cuervo, 2010). In contrast, extensively oxidized proteins aggregate to form an “inclusion-like” body the aggresome, which is located in the cytosol at the microtubule-organizing center and which actively sequesters insoluble proteins (Kopito, 2000; Kaganovich et al., 2008). These aggregates can be sequestered into the nascent autophagosome by a series of cargo-recognition proteins and cytosolic chaperones, and are then transported to the late endosomes and lysosomes by macroautophagy (Kopito, 2000; Kaganovich et al., 2008; Lamark, T., 2009). Additionally, extracellular oxidized matrix and aggregates from apoptotic cells (apoptotic bodies) are delivered to endosomal compartments following phagocytosis by tissue resident macrophages and DC (Chiti et al., 2006; Alavez et al., 2011; Devitt et al., 2011).

In the endosomes, oxidatively damaged biomolecules are degraded to their constitutive amino acids by acidic endopeptidases. However, heavily oxidized proteins, cross-linked by disulphide bonds, aggregate into a mixture of protein lipid deposits which are often inaccessible to lysosomal hydrolases (Chiti et al., 2006; Dunlop et al., 2009; David et al., 2010; Tyedmers et al., 2010). These aggregates can further enlarge over time by the addition of newly oxidized molecules, and induce endosomal destabilization and cytotoxic cell death (Dunlop et al., 2009).

Immunosenescence is characterized by a decreased ability of the immune system to respond to foreign antigens, as well as a decreased ability to maintain tolerance to self-antigens. This results in an increase susceptibility to infection and cancer, and reduced responses to vaccination (Linton et al., 2004; Agrawal et al., 2007; Pawelec et al., 2010; Shaw et al., 2010). Innate immune responses such as phagocytosis, ROS production and TLR function are generally compromised during immunosenescence (Bruunsgaard et al., 2000; de la Fuente et al., 2004; Nomellini et al., 2008; Agrawal et al., 2010; Fujimoto et al., 2010). Likewise, adaptive immune responses are hindered by a decrease in the variety of the B and T cell repertoire, as well as their ability to clonally expand following antigen stimulation (Fratelli et al., 2002; Larbi et al., 2007). Some controversy exists as to the capacity of DC from aging mice to stimulate T and B cells. In mice there is a general agreement that splenic and nodal common DC are impaired in their capacity to stimulate a proliferative response or to induce an anti-tumor immune response (Sharma et al., 2006). However, in aging subjects there is more disagreement. Some authors report a normal ability of DC to stimulate T cells (Grewe et al., 2001) whereas others report that DC purified from elderly subjects can activate memory but not naïve T cells (Agrawal et al., 2007). With regard to cytokine and chemokine production, several reports indicate a general dysregulation with aging, with a low level chronic production of pro-inflammatory cytokines associated with decreased responsiveness to cytokine production following specific stimuli (Bruunsgaard et al., 2000; de la Fuente et al., 2004; Nomellini et al., 2008; Cannizzo et al., 2011).

In this report, using biochemical and biophysical techniques, we present evidence that in DC purified from aging mice the exogenous and endogenous antigen processing and presentation pathways are impaired. Two major biochemical mechanisms can explain the impaired antigen processing and presentation ability of DC from aging mice: (i) the overall oxidative proteome could compromise the functionality of membrane organelles and cellular pathways associated with the antigen processing and loading machinery, or (ii) the overloading of endosomal compartments with oxidatively damaged proteins and protein/lipid micro-aggregates could interfere with efficient endosomal proteostasis (Stadtman, 1992; Cloos et al., 2004; Stadtman, 2004; Dunlop et al., 2008; Dunlop et al., 2009; Tyedmers et al., 2010). In favor of the first hypothesis are the data derived from the MS/MS mapping of the cellular oxidative proteome, which indicates that, indeed, proteins associated with many cellular pathways involved in protein trafficking, mitochondrial ATP generation and overall cellular basic functions are oxidized. A question still lingering is the relationship between amino acid oxidation and protein loss of biological activity (Stadtman, 1992; Cloos et al., 2004; Stadtman, 2004; Dunlop et al., 2008; Dunlop et al., 2009). In principle, the number of oxidative moieties on a protein, directly correlate with the loss of biological function, since carbonylation is an irreversible post-translational modification and the higher the oxidation state the higher is the likelihood that the protein would irreversibly unfold and lose its biological function. Additionally, oxidized proteins are targeted for degradation, and specific oxidations on specific amino acids can have a different impact on protein proteolysis directly increasing or decreasing the protein half life. For example, L-dopa modified proteins generate high molecular weight aggregates which are SDS-stable and resistant to proteolysis, and up-regulate the transcription and activity of endosomal cathepsins (S and L) (Rodgers et al., 2004). On the other hand, hydroxylation of the same amino acids results in increased protein catabolism (Dunlop et al., 2009). Currently we do not know the level of oxidation, the half life and the residual biological activity for each of the proteins we identified by MS/MS as oxidatively modified and which are involved in antigen processing and presentation. However, we present evidence that a decrease in their level of oxidation increases the overall ability of DC to process and present immunizing peptides (Rudensky et al., 1991; Murphy et al., 1992; Itano et al., 2003).

The second hypothesis is that overloading of endosomal compartments with oxidatively damaged proteins as well as micro-aggregates could interfere with efficient antigen processing. In favor of this hypothesis we demonstrate that MHC class II positive late endosomes do indeed accumulate protein micro-aggregates, which are greatly diminished by *in vivo* treatment with antioxidant.

At the present time we do not favor any of the two hypotheses and we actually consider it more likely that oxidative stress compromises both the functionality of proteins involved in antigen processing and presentation as well as interferes with endosomal proteostasis following accumulation of insoluble protein aggregates, which hijack cathepsin activity as previously shown in other aging cells (Rodgers et al., 2004).

Finally, conventional DC have a short half life and are constantly replaced by bone marrow derived circulating elements. Herein we demonstrated that in aging mice, despite their short life span, these cells accumulate products of oxidative damage, likely because they are derived from an “aging bone marrow” which contains precursor elements already compromised by oxidative stress. This hypothesis is sustained by our results which indicate increased presence of carbonylated proteins in CD34⁺ cells freshly purified from 22 month old mice. Additionally, the increased amount of aging-associated ROS in each parenchymal organ could further the cellular damage of newly generated DC. The short life span of DC could also be the main reason of why the *in vivo* therapy with antioxidant scavengers proved to be so effective. In fact by treating the mice for two weeks with an antioxidant we could

reduce the amount of carbonylated proteins in the newly generated DC and increase the cells overall biological performance, something that could not be attainable in cells with a much longer life-span.

Taken together, our analysis reports in a qualitative and quantitative manner the presence of increased protein carbonylation, glycation and lipoxidation in DC purified from lymphatic organs of aging mice. Micro-aggregates of oxidatively damaged proteins were found in endosomal compartments likely transported by autophagic pathways (Cuervo, 2010; Sahu et al., 2011). The data support the conclusion that age-related oxidative stress interferes with the ability to mount an MHC class II restricted immune response, and that this function can be partially restored following in vivo antioxidant therapy.

Experimental Procedure

Mice and mice treatments

C57BL/6J and CBA mice (3, 12 and 22 month old) were purchased from Harlan as part of the age-controlled NIH mouse colony program. All animal procedures were carried out according to a protocol approved by the Institutional Animal Care of Albert Einstein College of Medicine. In some experiments mice were injected in the flanks with 50 μ g of E α -RFP protein and inguinal lymph nodes collected after 6 or 24 hours. In other experiments mice were immunized in the flanks and nape of the neck with 100 μ g of E α -RFP protein in complete Freund's adjuvant and axillary and inguinal lymph nodes harvested two weeks later. In other experiments, following immunization mice received a single i.p injection of ammonium pyrrolidine dithiocarbamate (PDTC, Sigma, St. Louis, MO) (50 mg/kg), followed by oral PDTC treatment (5 mg/ml in drinking water) for two weeks. In some experiments (Figure 4f, 4g) splenic DC were expanded in vivo, to obtain a sufficient number of cells for MHC II peptide elution. Mice were injected subcutaneously with the B16-FLT3L line. Spleens were collected after 2 weeks.

Preparation of E α -RFP and HEL-FITC

E α -RFP (Itano et al., 2003) protein expression plasmid was generously provided by Denzin Lisa (Memorial Sloan Kettering, New York). Protein production was induced with 1 mM IPTG for 48 h, and the E α -RFP protein purified from the bacterial lysate using a Ni²⁺-charged His-Bind resin column (Novagen, EMD chemicals Gibbson, NJ) followed by FPLC purification. Protein expression and purity was assessed by SDS-PAGE followed by silver staining. Five milligrams of HEL (hen egg lysozyme) (>98% purity Sigma-Aldrich), were incubated with 200 μ l of FITC solution (stock 10 mg/ml in DMSO) in sodium bicarbonate buffer (pH>8.0-9.0) at room temperature for 1 hour. The free dye was removed from the labeled protein by dialysis. The total amount of labeled protein was calculated with the following formula (moles/L= [A280-(A494x0.3)] \times dilution factor]/38,940; where 38,940 is the molar extinction coefficient (moles-1cm-1) for the dye). On average 5-10 FITC molecules/protein were incorporated.

T cell proliferation

Inguinal and axillary lymph nodes were harvested two weeks after immunization and 6×10^5 cells seeded in a 96 well plate with or without titrated amounts of the immunizing antigen for 72 hours. Thymidine (1 μ Cu) was added 18 hours before cell harvesting. Cells were harvested on a Tomtec harvester (Model 94-3-468) and incorporated thymidine counted on a liquid scintillation counter (1450 Microbeta Wallac Trilux).

Flow Cytometry

Nodal or splenic purified DC were incubated for 30 minutes on ice with saturating amounts of anti-Y-Ae Alexa-647 (gift from Lisa Denzin, Memorial Sloan Kettering) AW3.1-FITC (gift from Emil Unanue, Washington University) rat anti mouse IA/IE (clone M5114, Pharmingen) or I-A^b-CLIP (gift from Paul Roche NIH) in staining buffer (PBS, 0.1% BSA, 0.01% NaN₃). Following washing in staining buffer, samples were analyzed with the FACScan flow cytometer (Becton Dickinson, N.J, USA).

Antigen processing Assay

CD11c⁺ DC, purified by magnetic beads immunoselection (Miltenyi Biotec) were pulsed with 20 microgram of E α -RFP or HEL-FITC for 1 hour. Cells were then washed in PBS and chased for different time points. After collection DC were analyzed by FACS to detect processing of E α -RFP or HEL-FITC proteins as well as MHC class II loading I-A^b/E α -52-68 and I-A^k/HEL-48-61.

Western blot analysis

List of antibodies and procedure are reported in Supplement Materials and methods

Fluorescence microscopy

CD11c⁺ DC were grown on coverslips, fixed for 10 minutes in either ice-cold methanol or 4% formaldehyde in PBS, blocked and permeabilized (1% BSA, 2% new-born calf serum, 0.01% Triton X-100), and then incubated with the primary LC3 and corresponding Alexa 488 or cyanine 5-conjugated secondary antibodies as described previously (Kaushik et al., 2006). After immunostaining, cells were rinsed with PBS and mounted for microscopy using Fluoromount-G (Southern Biotech). Images were collected using an Axiovert 200 fluorescence microscope (Carl Zeiss) equipped with a $\times 63$ objective, 1.4 numerical aperture and ApoTome. Quantification was performed on images with maximum projection of all Z-stack sections using ImageJ (NIH) after thresholding. Particle number was quantified with the “analyze particles” function in thresholded images with size (pixel²) settings from 0.1-10 and circularity 0-1. Where indicated, cells were incubated with MitoTracker (Molecular Probes) for 15 min, or BSA for 30 min, rinsed with PBS and processed for immunofluorescence as detailed above.

Endosomal subcellular fractionation and E α -RFP vitro processing

Splenic CD11c⁺ DC purified from 3, 12 and 22 month old mice, previously injected with the B16-FLT3L line, were collected, homogenized and then fractionated on consecutive Percoll gradient (27 and 10 %) as previously described (Sahu et al., 2011). Ten microgram of late endosomes, from each age group, were incubated with five micrograms of E α -RFP in 120 mM Na-acetate pH 5 at 37 °C. After 30 minutes samples were collected and run on a 12 % SDS-PAGE. E α -RFP digestion was monitored by silver staining (Pierce Silver Staining Kit, Thermo scientific).

LTDQ-tandem MS/MS sequencing

Three sets of experimental samples were analyzed by MS/MS; i) DNPH immunoprecipitate of oxidized proteins (Figure 1g, 1h, 2a and Supplement Table 1 and table 2) ii) samples derived from E α -RFP processing by purified endosomal compartments (Figure 5e) and iii) samples eluted from surface MHC II proteins from DC of 3, 12 and 22 months old mice immunized with E α -RFP (4f, 4g). Following incubation at 37°C with purified endosomal compartments the reaction was stopped with 0.5 % TFA. Processed and MHC class II eluted peptides were retrieved by filtration through 10 kDa Millipore devices and subjected to MS/MS peptide sequencing. Purified splenic DCs from 3, 12 and 22 month mice were lysed and

subjected to DNPH immunoprecipitation of carbonyl modified proteins. The eluted samples were run on a 10% SDS-PAGE. The gel was silver stained and the proteins were excised from both the stacking and the resolving part of the gel. LTQ-MS/MS sequencing was performed using a Nanospray LC-MS/MS on a LTQ linear ion trap mass spectrometer (LTQ, Thermo, San Jose, CA) interfaced with a TriVersa NanoMate nanoelectrospray ion source (Advion BioSciences, Ithaca, NY).

Statistical analysis

Numerical results are reported as mean + SE. Data derived from a minimum of three independent experiments unless stated otherwise. Statistical significance of the difference between experimental groups, in instances of multiple means comparisons, was determined using one-way analysis of variance (ANOVA), followed by the Bonferroni post hoc test. Differences were considered significant for $p < 0.05$.

Supplementary Material

Refer to Web version on PubMed Central for supplementary material.

Acknowledgments

This work was supported by the National Institutes of Health Grants AI48833 to L.S. and AG031782, DK041918 to A.M.C. F.M. and L.S., and a National Institute on Aging Training Grant (S.K.). LNA was supported by the NIH Fogarty Geographic Infectious Diseases Training Grant D43TW007129. None of the authors on this manuscript have a financial interest related to this work.

References

- Agrawal A, Agrawal S, Gupta S. Dendritic cells in human aging. *Exp. Gerontol.* 2007; 42:421–426. [PubMed: 17182207]
- Agarwal S, Busse PJ. Innate and adaptive immunosenescence. *Ann. Allergy Asthma Immunol.* 2010; 104:183–190. [PubMed: 20377107]
- Alexeyev MF. Is there more to aging than mitochondrial DNA and reactive oxygen species? *FEBS J.* 2009; 276:5768–5787. [PubMed: 19796285]
- Alavez S, Vantipalli MC, Zucker DJ, Klang IM, Lithgow GJ. Amyloid-binding compounds maintain protein homeostasis during ageing and extend lifespan. *Nature.* 2011; 472:226–229. [PubMed: 21451522]
- Arndt V, et al. Chaperone-assisted selective autophagy is essential for muscle maintenance. *Curr Biol.* 2010; 20:143–148. [PubMed: 20060297]
- Barja G, Herrero A. Oxidative damage to mitochondrial DNA is inversely related to maximum life span in the heart and brain of mammals. *FASEB J.* 2000; 14:312–318. [PubMed: 10657987]
- Broadley SA, Hartl FU. Mitochondrial stress signaling: a pathway unfolds. *Trends Cell Biol.* 2008; 18:1–4. [PubMed: 18068368]
- Brunsgaard H, Pedersen M, Klarlund B. Aging and proinflammatory cytokines. *Current Opinion in Hematology.* 2000; 8:131–116. [PubMed: 11303144]
- Cannizzo ES, Clement CC, Sahu R, Follo C, Santambrogio L. Oxidative stress, inflamm-aging and immunosenescence. *J. Proteomics.* 2011 in press.
- Cathcart MK. Regulation of superoxide anion production by NADPH oxidase in monocytes/macrophages: contributions to atherosclerosis. *Arterioscler. Thromb. Vasc. Biol.* 2004; 24:23–28. [PubMed: 14525794]
- Chandel NS. Mitochondrial regulation of oxygen sensing. *Adv. Exp. Med. Biol.* 2010; 661:339–354. [PubMed: 20204741]
- Chiti F, Dobson CM. Protein misfolding, functional amyloid, and human disease. *Annu. Rev. Biochem.* 2006; 75:333–366. [PubMed: 16756495]

- Cloos PA, Christgau S. Post-translational modifications of proteins: implications for aging, antigen recognition, and autoimmunity. *Biogerontology*. 2004; 5:139–158. [PubMed: 15190184]
- Cowan KJ, Diamond MI, Welch WJ. Polyglutamine protein aggregation and toxicity are linked to the cellular stress response. *Hum. Mol. Genet.* 2003; 12:1377–1391. [PubMed: 12783846]
- Cuervo AM, et al. Autophagy and aging: the importance of maintaining “clean” cells. *Autophagy*. 2005; 1:131–140. [PubMed: 16874025]
- Cuervo AM. Chaperone-mediated autophagy: selectivity pays off. *Trends Endocrinol Metab.* 2010; 21:142–150. [PubMed: 19857975]
- Dale DC, Boxer L, Liles WC. The phagocytes: neutrophils and monocytes. *Blood*. 2008; 112:935–945. [PubMed: 18684880]
- Dalle-Donne I, Rossi R, Giustarini D, Milzani A, Colombo R. Protein carbonyl groups as biomarkers of oxidative stress. *Clin Chim Acta.* 2003; 329:23–38. [PubMed: 12589963]
- de la Fuente M, Hermanz A, Guayerbas N, Alvarez P, Alvarado C. Changes with age in peritoneal macrophage functions. Implication of leukocytes in the oxidative stress of senescence. *Cell. Mol. Biol.* 2004; 50:683–690.
- David DC, et al. Widespread protein aggregation as an inherent part of aging in *C. elegans*. *PLoS Biol.* 2010; 8:8–14.
- Devitt A, Marshall LJ. The innate immune system and the clearance of apoptotic cells. *J Leukoc Biol.* 2011; 5:67–73.
- Dufour E, Boulay J, Rincheval V, Sainsard-Chanet A. A causal link between respiration and senescence in *Podospora anserina*. *Proc Natl Acad Sci U S A.* 2000; 97:4138–4143. [PubMed: 10759557]
- Dunlop RA, Dean RT, Rodgers KY. The impact of specific oxidized amino acids on protein turnover in J774 cells. *Biochem. J.* 2008; 410:131–141. [PubMed: 17953511]
- Dunlop RA, Brunk UT, Rodgers KJ. Oxidized Proteins: Mechanisms of removal and consequences of accumulation. *Life.* 2009; 61:522–527. [PubMed: 19391165]
- Durieux J, Wolff S, Dillin A. The cell-non-autonomous nature of electron transport chain-mediated longevity. *Cell.* 2011; 144:79–91. [PubMed: 21215371]
- Dyer DG, et al. Accumulation of Maillard reaction products in skin collagen in diabetes and aging. *J Clin Invest.* 1993; 91:2463–249. [PubMed: 8514858]
- Fratelli M, et al. Identification by redox proteomics of glutathionylated proteins in oxidatively stressed human T lymphocytes. *PNAS.* 2002; 99:3505–3510. [PubMed: 11904414]
- Fujimoto H, Kobayashi H, Ohno M. Age-induce reduction in mitochondrial manganese superoxide dismutase activity and tolerance of macrophages against apoptosis induced by oxidized low density lipoprotein. *Circ. J.* 2010; 4:353–360. [PubMed: 20009389]
- Grewe M. Chronological ageing and photoageing of dendritic cells. *Clin Exp Dermatol.* 2001; 26:608–612. [PubMed: 11696065]
- Guptasarma P, Balasubramanian D, Matsugo S, Saito I. Hydroxyl radical mediated damage to proteins, with special reference to the crystallins. *Biochemistry.* 2002; 31:4296–4303. [PubMed: 1567875]
- Haigis MC, Yankner BA. The aging stress response. *Mol. Cell.* 2010; 40:333–344. [PubMed: 20965426]
- Halliwell B. The wanderings of a free radical. *Free Radic. Biol. Med.* 2009; 46:531–542. [PubMed: 19111608]
- Hamanaka RB, Chandel NS. Mitochondrial reactive oxygen species regulate cellular signaling and dictate biological outcomes. *Trends Biochem. Sci.* 2010; 35:505–513. [PubMed: 20430626]
- Hung LF, et al. Advanced glycation end products induce T cell apoptosis: Involvement of oxidative stress, caspase and the mitochondrial pathway. *Mech. Aging Dev.* 2010; 131:682–961. [PubMed: 20888855]
- Isom AL, et al. Modification of Cytochrome c by 4-hydroxy- 2-nonenal: evidence for histidine, lysine, and arginine-aldehyde adducts. *J Am Soc Mass Spectrom.* 2004; 15:1136–1147. [PubMed: 15276160]

- Itano AA, et al. Distinct dendritic cell populations sequentially present antigen to CD4 T cells and stimulate different aspects of cell-mediated immunity. *Immunity*. 2003; 19:47–57. [PubMed: 12871638]
- Johnson F, Giulivi C. Superoxide dismutases and their impact upon human health. *Mol Aspects Med*. 2005; 26:340–352. [PubMed: 16099495]
- Kaganovich D, Kopito R, Frydman J. Misfolded proteins partition between two distinct quality control compartments. *Nature*. 2008; 454:1088–1095. [PubMed: 18756251]
- Klebanoff SJ. Myeloperoxidase: friend and foe. *J. Leukoc. Biol*. 2005; 77:598–625. [PubMed: 15689384]
- Kopito RR. Aggresomes, inclusion bodies and protein aggregation. *Trends Cell Biol*. 2000; 10:524–530. [PubMed: 11121744]
- Lamark T, Kirkin V, Dikic I, Johansen T. NBR1 and p62 as cargo receptors for selective autophagy of ubiquitinated targets. *Cell Cycle*. 2009; 8:1986–1990. [PubMed: 19502794]
- Larbi A, Dupuis G, Douziech N, Khalil A, Fulop T. Low-Grade Inflammation with Aging Has Consequences for T-Lymphocyte Signaling. *Ann. N. Y. Acad. Sci*. 2004; 1030:125–133. [PubMed: 15659789]
- Larbi A, Kempf J, Pawelec G. Oxidative Stress modulation and T cell activation. *Experimental Gerontology*. 2007; 42:995–1002. [PubMed: 17611062]
- Lin MT, Beal MF. Mitochondrial dysfunction and oxidative stress in neurodegenerative diseases. *Nature*. 2006; 443:787–795. [PubMed: 17051205]
- Linton PJ, Dorshkind K. Age-related changes in lymphocyte development and function. *Nat. Immunol*. 2004; 5:133–139. [PubMed: 14749784]
- Madian AG, Regnier FE. Proteomic identification of carbonylated proteins and their oxidation sites. *J Proteome Res*. 2010; 9:3766–3780. [PubMed: 20521848]
- Murphy DB, et al. Monoclonal antibody detection of a major self peptide MHC class II complex. *J Immunol*. 1992; 148:3483–3491. [PubMed: 1375245]
- Nomellini V, Gomez C, Kovacs E. Aging and impairment of innate immunity. *Trends in Innate Immunity*. 2008; 15:188–205.
- Oliver CN, Ahn BW, Moerman EJ, Goldstein S, Stadtman ER. Age-related changes in oxidized proteins. *J Biol Chem*. 1987; 262:5488–5491. [PubMed: 3571220]
- Park JB. Phagocytosis induces superoxide formation and apoptosis in macrophages. *Exp. Mol. Med*. 2003; 35:325–335. [PubMed: 14646585]
- Pawelec G, Derhovanessian E, Larbi A. Immunosenescence and cancer. *Crit. Rev. Oncol. Hematol*. 2010; 75:165–172. [PubMed: 20656212]
- Ponnappan S, Ovaa H, Ponnappan U. Lower expression of catalytic and structural subunits of the proteasome contributes to decreased proteolysis in peripheral blood T lymphocytes during aging. *Int. J. Biochem. Cell. Biol*. 2007:799–809. [PubMed: 17317272]
- Preynat-Seauve O, Coudurier S, Favier A, Marche PN, Villiers C. Oxidative stress impairs intracellular events involved in antigen processing and presentation to T cells. *Cell Stress Chaperones*. 2003; 8:162–171. [PubMed: 14627202]
- Requena JR, Chao CC, Levine RL, Stadtman ER. Glutamic and amino adipic semialdehydes are the main carbonyl products of metal-catalyzed oxidation of proteins. *PNAS*. 2001; 98:69–74. [PubMed: 11120890]
- Roberts CK, Sindhu KK. Oxidative stress and metabolic syndrome. *Life Sci*. 2009; 84:705–712. [PubMed: 19281826]
- Rodgers KJ, Hume PM, Dunlop RA, Dean RT. Biosynthesis and turnover of DOPA-containing proteins by human cells. *Free Radic Biol Med*. 2004; 37:1756–1764. [PubMed: 15528035]
- Rudensky A, et al. Sequence analysis of peptides bound to MHC class II molecules. *Nature*. 1991; 353:622–627. [PubMed: 1656276]
- Sacksteder CA, et al. Endogenously nitrated proteins in mouse brain: links to neurodegenerative disease. *Biochemistry*. 2006; 45:8009–8022. [PubMed: 16800626]
- Sahu R, et al. Microautophagy of cytosolic proteins by late endosomes. *Dev. Cell*. 2011; 20:131–139. [PubMed: 21238931]

- Sharma S, Dominguez AL, Lustgarten J. Aging affect the anti-tumor potential of dendritic cell vaccination, but it can be overcome by co-stimulation with anti-OX40 or anti-4-1BB. *Exp Gerontol.* 2006; 41:78–84. [PubMed: 16289924]
- Shaw AC, Joshi S, Greenwood H, Panda A, Lord JM. Aging of the innate immune system. *Curr. Opin. Immunol.* 2010; 22:507–513. [PubMed: 20667703]
- Squier TC. Oxidative stress and protein aggregation during biological aging. *Exp. Gerontology.* 2001; 36:1539–1550.
- Stadtman ER. Protein oxidation and aging. *Science.* 1992; 257:1220–1224. [PubMed: 1355616]
- Stadtman ER. Role of oxidant species in aging. *Curr Med Chem.* 2004; 11:1105–1112. [PubMed: 15134509]
- Starkov AA, et al. Mitochondrial alpha-ketoglutarate dehydrogenase complex generates reactive oxygen species. *J Neurosci.* 2004; 24:7779–7788. [PubMed: 15356189]
- Stern LJ, Potoicchio I, Santambrogio L. MHC class II compartment subtypes: structure and function. *Current Opinion in Immunology.* 2006; 18:64–69. [PubMed: 16337363]
- Takahashi M, et al. Oxidative stress-induced phosphorylation, degradation and aggregation of alpha-synuclein are linked to upregulated CK2 and cathepsin D. *Eur J Neurosci.* 2007; 26:863–874. [PubMed: 17714183]
- Terman A. Catabolic insufficiency and aging. *Ann. N. Y. Acad. Sci.* 2006; 1067:27–36. [PubMed: 16803967]
- Toda T, et al. Proteomic approaches to oxidative protein modifications implicated in the mechanism of aging. *Geriatr. Gerontol. Int.* 2010; 10:S25–31. [PubMed: 20590839]
- Tyedmers J, Mogk A, Bukau B. Cellular strategies for controlling protein aggregation. *Nat. Rev. Mol. Cell. Biol.* 2010; 11:777–788. [PubMed: 20944667]
- Wellen KE, Thompson CB. Cellular metabolic stress: considering how cells respond to nutrient excess. *Mol. Cell.* 2010; 40:323–332. [PubMed: 20965425]
- West XZ, et al. Oxidative stress induces angiogenesis by activating TLR2 with novel endogenous ligands. *Nature.* 2010; 467:972–976. [PubMed: 20927103]

- Aging Dendritic Cells are characterized by an oxidatively modified proteome.
- Aggregates of oxidized proteins accumulate in endosomal compartments.
- The oxidatively damaged proteome compromises DC ability to process and present MHC class II restricted antigens.
- Antioxidant treatment, partially restore DC's priming ability only in aging mice.

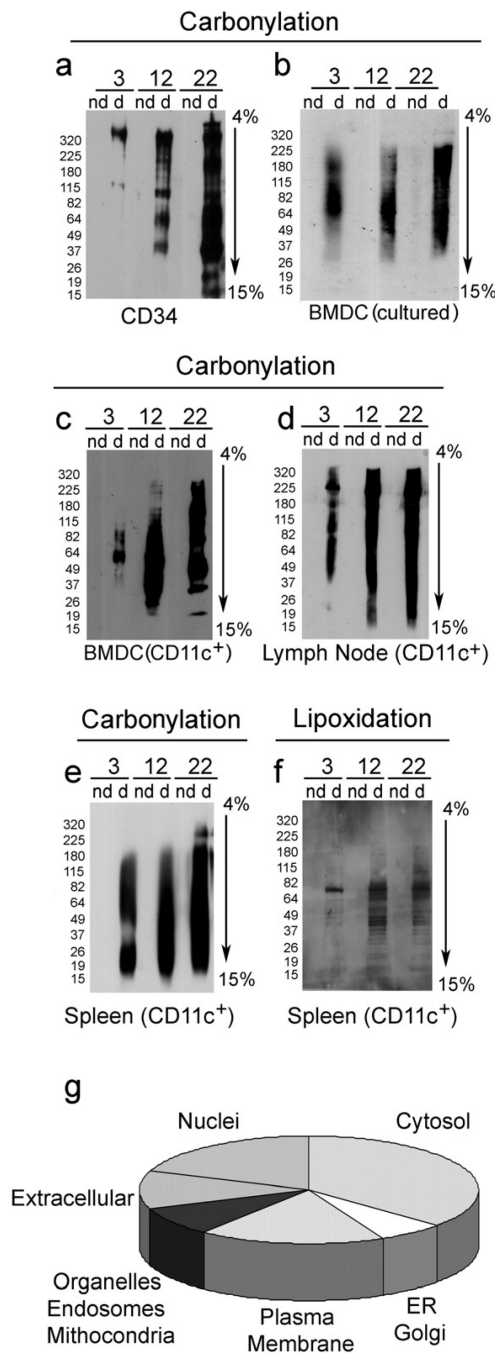


Figure 1. Detection of oxidatively modified proteins in DC purified from primary and secondary lymphatic organs

a,b,c,d,e Western blot analysis of carbonylated proteins detected in **a**) purified CD34⁺ bone marrow precursors **b**) bone marrow dendritic cells (BMDC) cultured in GM-CSF for 7 days and **c,d,e**) conventional CD11c⁺ DC freshly purified from primary and secondary lymphatic organs from 3, 12, and 22 month old mice. One representative experiment out of four is shown. **f**) Western blot analysis of lipoxidated proteins (probing for malondialdehyde) detected in conventional CD11c⁺ freshly purified splenic DC. Lanes marked as (d) report derivatized proteins and (nd) report non-derivatized proteins (specificity control). Loading controls are reported in Supplement Figure 1. **g**) Pie chart reporting the subcellular

distribution of the oxidative proteome immunoprecipitate from conventional CD11c⁺ splenic DC purified from 22 month old mice.

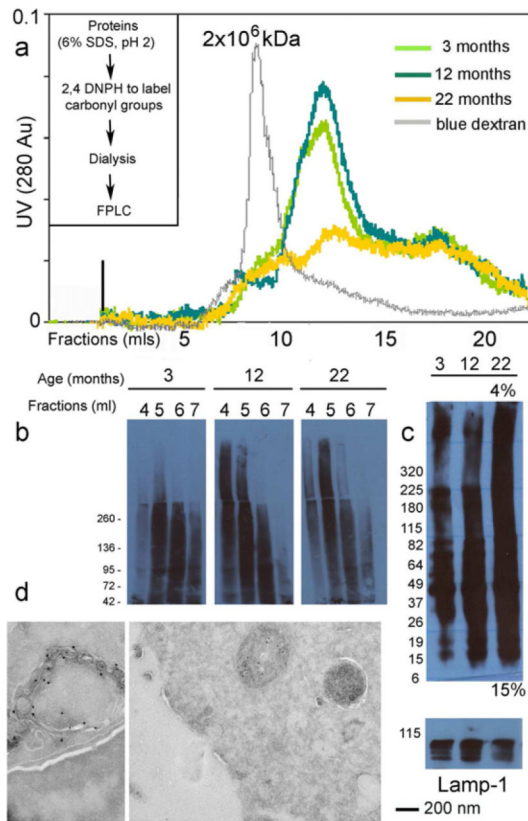


Figure 2. Accumulation of micro aggregates of oxidatively damaged proteins in splenic DC purified from aging mice

a) FPLC separation of micro-aggregates of carbonylated proteins derived from CD11c⁺ splenic DC purified from 3, 12, and 22 month old mice. One preparation, out of two is shown. **b)** Western blot analysis of the FPLC high molecular weight fractions to detect micro-aggregates of oxidized proteins. Total cell lysates were prepared from CD11c⁺ splenic DC purified from the spleen of 3, 12 and 22 month old mice. One preparation, out of two is shown. **c)** Western blot analysis of carbonylated proteins detected in late endosomal compartments, gradient-purified from splenic DC of 3, 12 and 22 month old mice. LAMP1 immunoblot is shown as a loading control. **d)** Ultrastructural morphology of late endosomal multivesicular bodies (MVBs) from CD11c⁺ splenic DC purified from a 22 month old mice. Immunogold labeling for MHC class II molecules (Ab clone AF120.6 is 5 nm gold and Ab clone M5-114 is 10 nm gold).

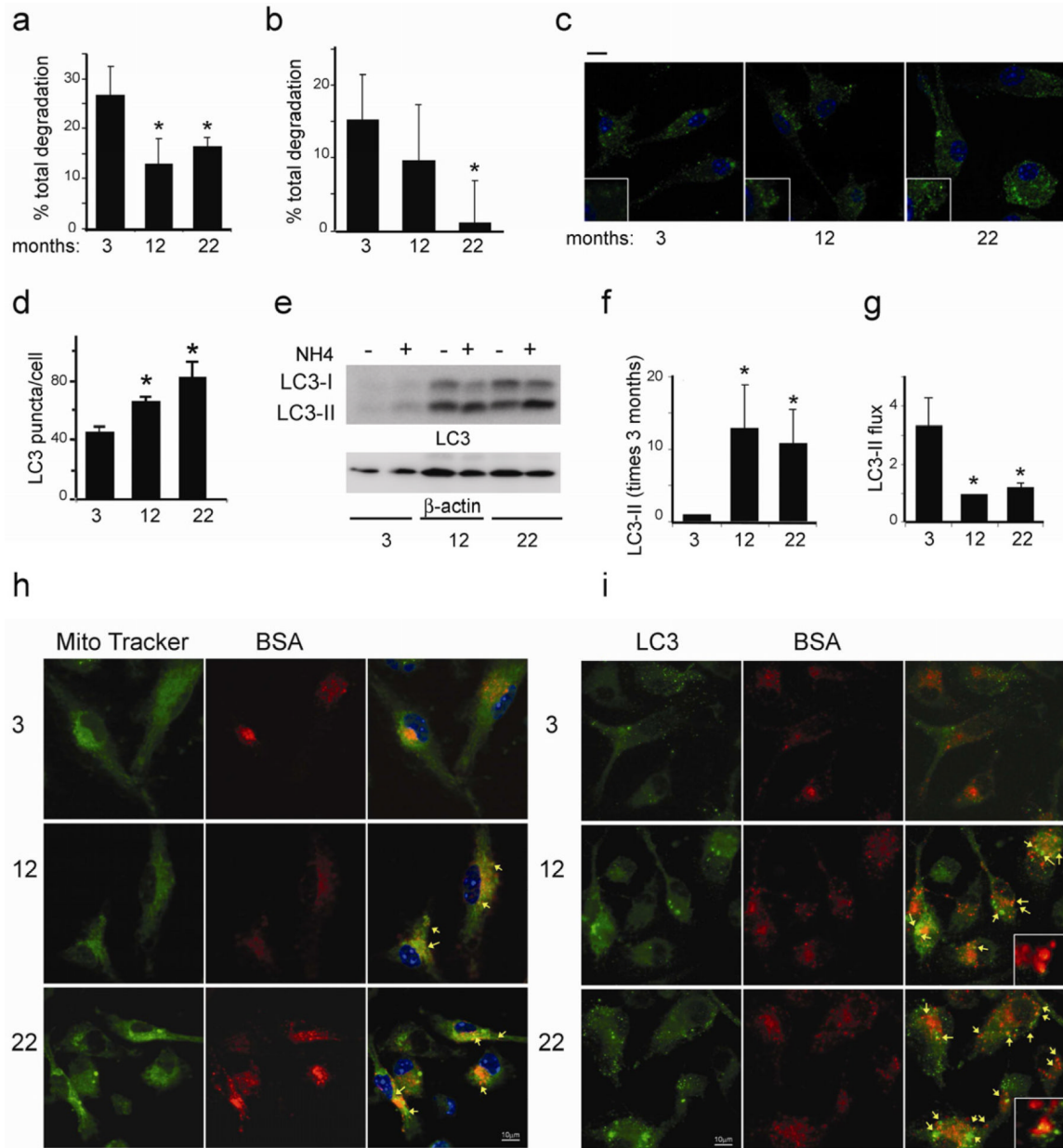


Figure 3. Decreased endosomal/lysosomal degradation and compromised macroautophagy in DC from aging mice

a, b) CD11c⁺ splenic DC purified from 3, 12 and 22-month mice were labeled for 2 days with [³H]leucine. During the chase cells were maintained for 24 hours in the presence or absence of NH₄Cl/leupeptine (**a**) or 3Methyl-adenine (**b**) to block all lysosomal proteolysis or macroautophagy, respectively. Proteolysis rates for long lived proteins after a 20h chase are shown. Values are the mean ± S.D. of three different experiments with triplicate wells. * indicate a p value < 0.05. **c**) Immunofluorescence analysis of LC3 distribution in CD11c⁺ splenic DC from 3, 12 and 22 month old mice. **d**) Quantification of the number of LC3-positive puncta per cell. * indicate a p value < 0.05 **e, f, g**) LC3 flux in CD11c⁺ splenic DC from 3, 12 and 22-month mice. Cells were incubated in the presence or absence of lysosomal protease inhibitors (PI) for 2h, collected and subjected to SDS-PAGE and immunoblot for LC3. **e**) Representative immunoblot. **f**) Quantification of steady-state levels

of LC3-II (content of autophagic vacuoles (AV)) and **g**) LC3 flux (ratio of LC3-II in the presence and absence of protease inhibitors. * indicate a p value < 0.05. **h, i**) Immunofluorescence of CD11c⁺ splenic DC from 3, 12 and 22-month mice **h**) incubated with BSA-biotin and mitotracker or **i**) incubated with BSA and immunostained for LC3 . Panels show individual channels and merged images. Arrows indicate points of convergence of the different fluorophores.

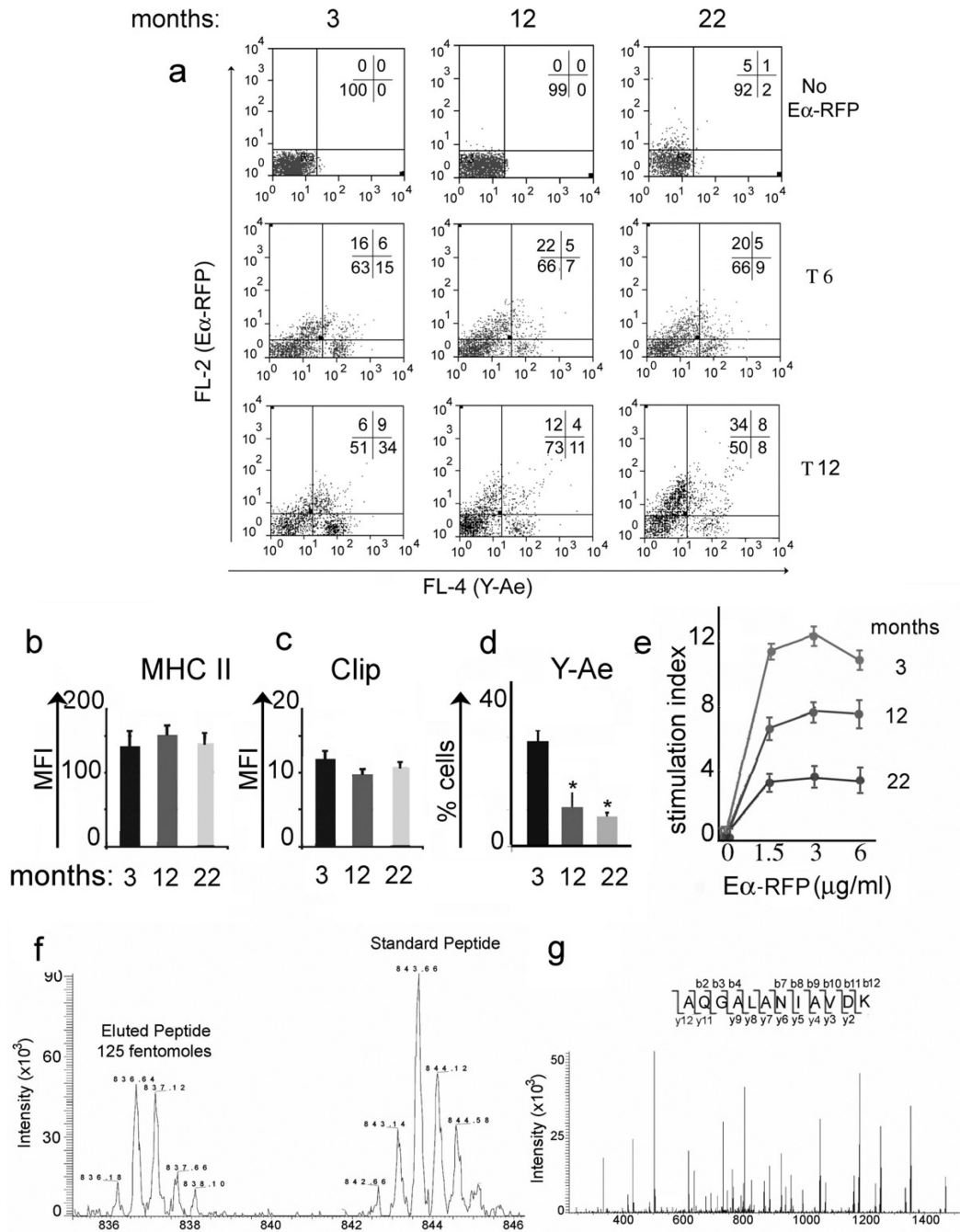


Figure 4. Decreased *in vivo* endosomal processing and MHC class II restricted presentation in conventional CD11c⁺ DC from aging mice

a) FACS analysis of CD11c⁺ splenic DC, purified from 3, 12 and 22 months old C57/Bl6 mice, following *in vivo* injection of Eα-RFP protein. Mice were injected with 50 μg/ml of Eα-RFP. CD11c⁺ DC were purified from the popliteal node and analyzed at different time points for RFP fluorescence, to quantify Eα-RFP processing, and Y-Ae staining to quantify I-Ab loading with the processed Eα 52-68 peptide. One representative experiment, out of three is shown. **b, c)** Bar graph of the mean fluorescence index and standard deviation of **b)** total surface MHC class II protein (I-A^b) and **c)** CLIP detected on the same CD11c⁺ DC population. **d)** Bar graph and standard deviation of the percentage of CD11c⁺ cells, which

stained with the Y-Ae antibody (specific for I-A^b/Ea 52-68 complex). * indicate a p value < 0.05. Lymph nodal CD11c⁺ DC were purified from 3, 12 and 22 month old mice, immunized with 100 µg of Ea-RFP in CFA, two weeks earlier. **e)** T cell proliferative response from lymph nodes harvested from 3, 12 and 22 month old mice, previously immunized with 100 µg of Ea in CFA (one out of four experiments is shown). **f)** Quantitative MS scan of the immunodominant Ea 52-68 peptide eluted from nodal CD11c⁺ DC purified from 3 month old mice previously immunized with 100 µg of Ea-RFP in CFA. Isotopically labeled Ea 52-68 peptide was spiked in the eluate for comparative quantification. One out of two quantification is reported. **g)** MS/MS fragmentation of Ea 52-68 peptide eluted from nodal CD11c⁺ DC purified from 3 month old mice previously immunized with 100 µg of Ea-RFP in CFA.

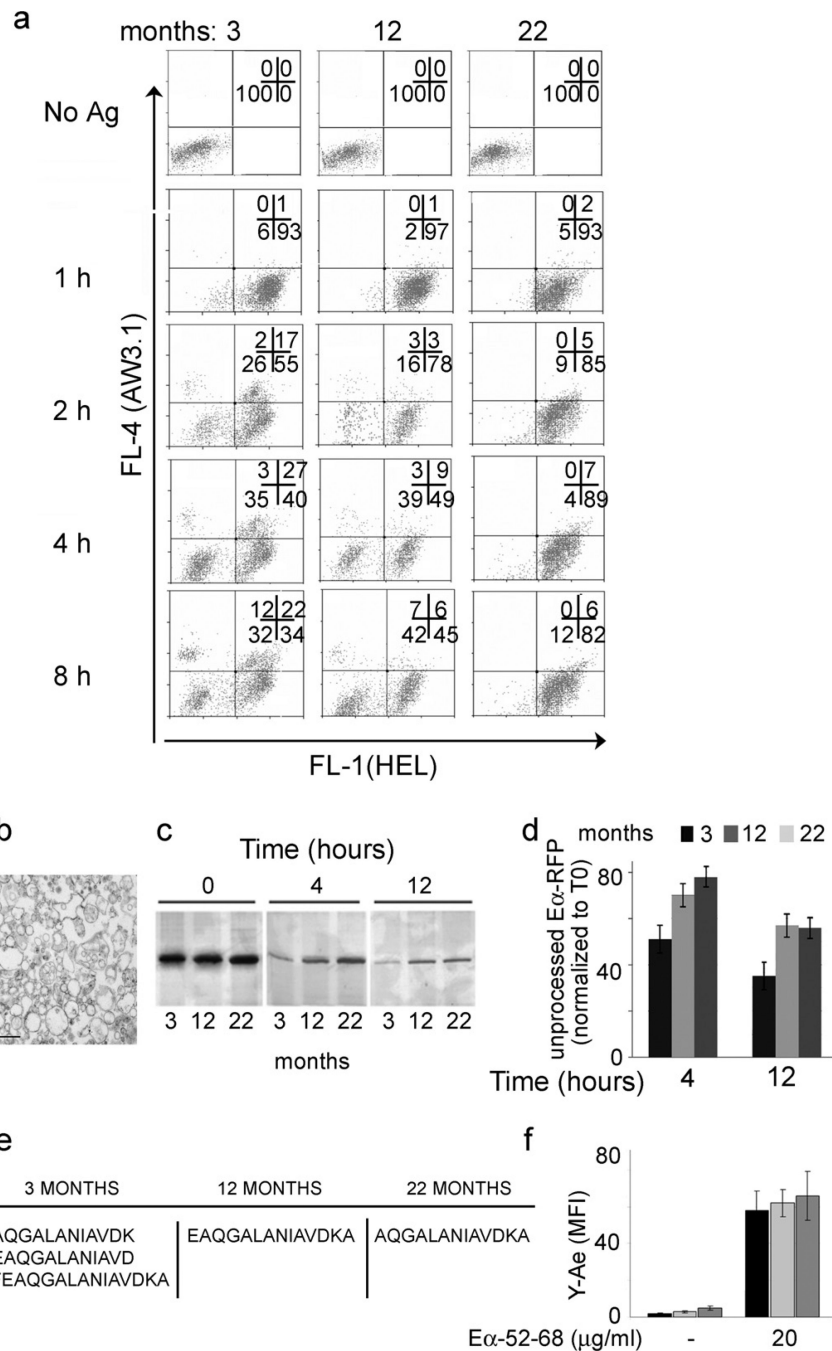


Figure 5. Decreased *in vitro* endosomal processing and MHC class II restricted presentation in conventional DC from aging mice

a) FACS analysis of CD11c⁺ splenic DC purified from 3, 12 and 22 months old CBA mice, following phagocytosis of HEL-FITC protein. DC were incubated with 20 μ g/ml of HEL-FITC protein (time 0). Cells were then chased at different time points for FITC fluorescence, to quantify HEL-FITC processing and AW3.1 staining to quantify I-A^k loading with the processed HEL 48-62 peptide. One representative experiment, out of four is shown. **b)** Ultrastructural analysis of MVBs purified from CD11c⁺ splenic DC by a 10/27 percoll gradient. **c)** Silver stained SDS-PAGE, of gradient purified late endosomal compartments (3, 12 and 22-month mice) incubated for the indicated time points with 5 μ g of recombinant

E α -RFP protein. Bands correspond to the amount of undigested E α -RFP at the indicated time points. **d)** Bar graph and standard deviation of the densitometric analysis of three independent endosomal processing experiments as reported in c. Data indicate the amount of E α -RFP protein still unprocessed at different time points, calculated as percentage of total E α -RFP (time 0). **e)** Peptide sequences, identified by MS/MS analysis, following endosomal E α -RFP *in vitro* processing. Data are collected from two sets of separate mass spectrometry analysis. **f)** Bar graph of the mean fluorescence index of Y-Ae surface staining of CD11c⁺ splenic DC harvested from 3, 12 and 22 month old mice following incubation with or without E α 52-68 peptide. One experiment out of three is shown.

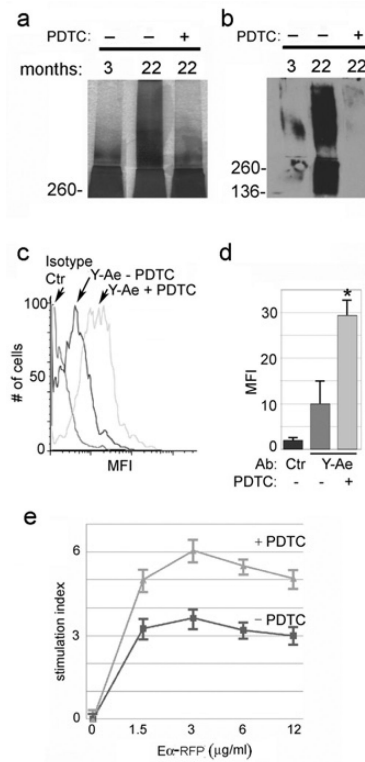


Figure 6. In vivo antioxidant treatment ameliorates MHC class II restricted immune response to immunizing antigen

a) Silver staining of protein micro-aggregates present in CD11c⁺ DC purified from the inguinal lymph nodes of 3 and 22 month old mice untreated (-) or treated (+) with the antioxidant agent PDTC. One out of three experiments is reported. **b)** Western blot analysis of carbonylated proteins present in CD11c⁺ DC purified from the inguinal lymph nodes of 3 and 22 month old mice, untreated (-) or treated (+) with the antioxidant agent PDTC. One out of three experiments is reported. **c)** Y-Ae surface staining of CD11c⁺ splenic DC harvested from 22 month old mice untreated (-) or treated (+) with the antioxidant agent PDTC for 2 weeks. After purification DC were pulsed for one hour with 20 μg of Eα-RFP and chased overnight before staining with Y-Ae. **d)** Bar graph depicting the average and standard deviation of Y-Ae staining collected as in (c) by four independent experiments). * indicate a p value < 0.05. **e)** T cell proliferative response from inguinal lymph nodes harvested from 22 month old mice, previously immunized with 100 μg of Eα in CFA, untreated (-) or treated (+) with the antioxidant agent PDTC for 2 weeks following immunization. One of four experiments is shown.

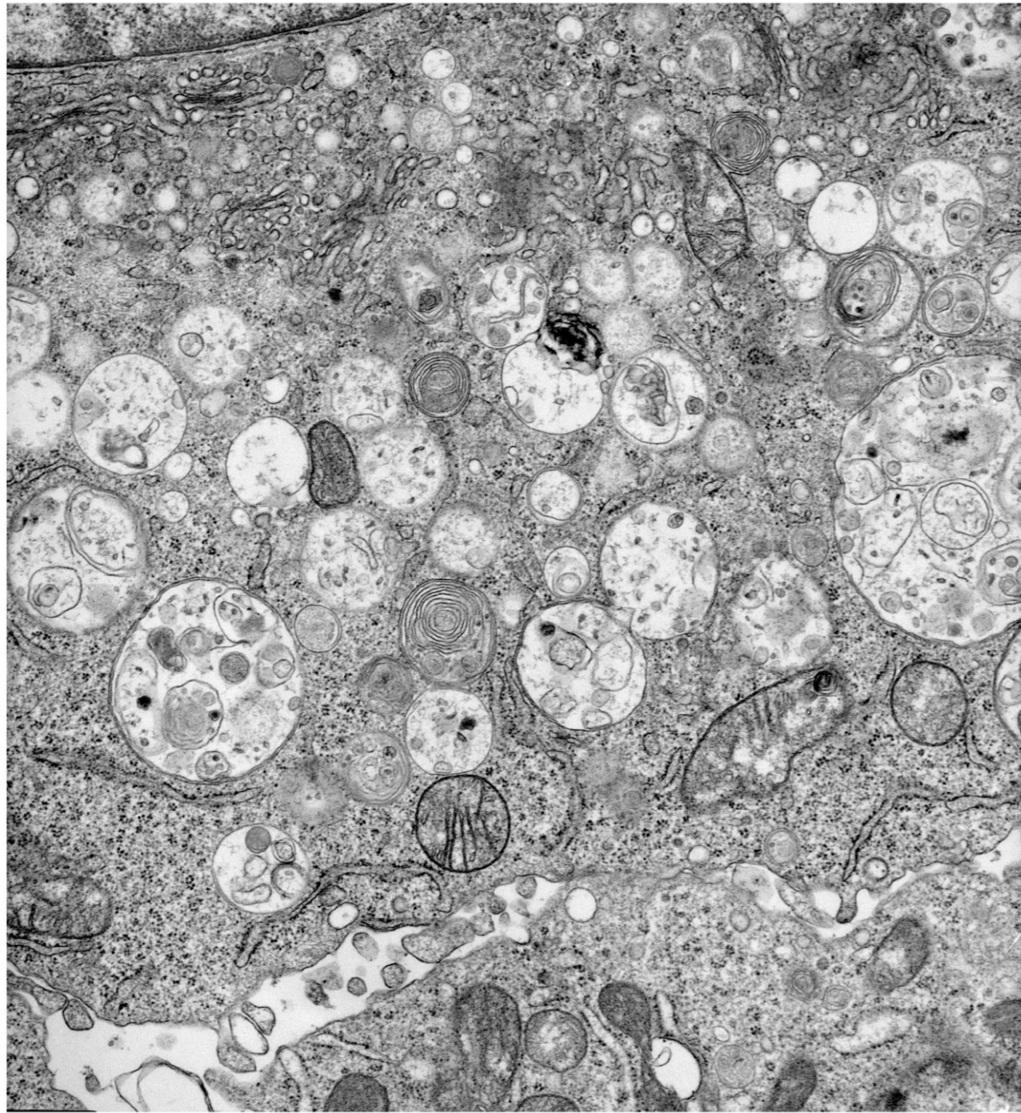


Table 1

Quantification of the number of amino acids (calculated from proteins listed in Supplement Table 1) with posttranslational oxidative modifications.

Amino acid	Chemical Modifications	%
Serine	Unmodified	91.5
	Glucuronyl	8.5
Cysteine	Unmodified	32.8
	Dioxidation (cysteine sulfinic acid)	35.7
	Trioxidation (cysteic acid)	31.5
Lysine	Unmodified	53.6
	Oxidation (hydroxy-Lys)	26.4
	Dioxidation (dihydroxy-Lys)	17.0
	Glucosylgalactosyl	3.0
Arginine	Unmodified	58.5
	Oxidation	21.6
	Dioxidation (hydroperoxide)	11.8
	3-deoxyglucosone (AGE derivative)	8.1
Tryptophan	Unmodified	30.0
	Oxidation (hydroxy-Trp/oxindolylalanine)	22.5
	Dioxidation (dioxindolylalanine/N-formylkynurenine)	13.5
	Kynurenin	13.5
	Oxolactone	16.5
	Hydroxykynurenin	4.0
Methionine	Unmodified	49.8
	Oxidation (Met-sulphoxide)	30.1
	Dioxidation	20.1
Tyrosine	Unmodified	87.2
	Oxidation (meta or ortho-hydroxy phenylalanine)	5.8
	Dioxidation (3,4 dihydroxy-phenylalanine (DOPA))	7.0
Phenylalanine	Unmodified	64.8
	Oxidation (meta or ortho-Tyrosine)	17.2
	Dioxidation (3,4 dihydroxy-phenylalanine (DOPA))	18.0
Proline	Unmodified	38.2
	Oxidation (hydroxy-proline)	37.6
	Dioxidation (dihydroxy-proline)	24.2
Aspartate	Unmodified	78.5
	Oxidation (hydroxy aspartic acid)	21.5
Histidine	Unmodified	85.0
	Oxidation (2-oxo-histidine)	15.0
Asparagine	Unmodified	81.9
	Oxidation	18.1